Surfactant free magnetic nanofluids based on core-shell type nanoparticle decorated multiwalled carbon nanotubes

Tessy Theres Baby and Ramaprabhu Sundara

Citation: Journal of Applied Physics **110**, 064325 (2011); doi: 10.1063/1.3642974
View online: http://dx.doi.org/10.1063/1.3642974
View Table of Contents: http://scitation.aip.org/content/aip/journal/jap/110/6?ver=pdfcov
Published by the AIP Publishing

Surfactant free magnetic nanofluids based on core-shell type nanoparticle decorated multiwalled carbon nanotubes

Tessy Theres Baby and Ramaprabhu Sundara[a)]
Alternative Energy and Nanotechnology Laboratory (AENL), Nano Functional Materials Technology Centre (NFMTC), Department of Physics, Indian Institute of Technology Madras, Chennai 600036, India

(Received 29 April 2011; accepted 14 August 2011; published online 27 September 2011)

Magnetic nanofluids consisting of fluids suspended with magnetic materials are of current interest and have potential applications in both energy related and biomedical fields. In this paper, we present a novel magnetic nanofluid obtained by dispersing silicon dioxide (SiO_2) coated on magnetite (Fe_3O_4) particle decorated multiwalled carbon nanotubes (MWNTs) (Fe_3O_4@SiO_2/MWNTs) in de-ionized water. As compared to a magnetite decorated MWNT based nanofluid, the present system shows better stability and thermal properties without the use of any surfactants. Fe_3O_4/MWNTs and Fe_3O_4@SiO_2/MWNTs have been synthesized via a simple chemical reduction technique and dispersed in de-ionized water via ultrasonication. Dispersed de-ionized water based nanofluids containing Fe_3O_4/MWNTs with surfactant and Fe_3O_4@SiO_2/MWNTs without surfactant show a thermal conductivity enhancement of 20% and 24.5%, respectively, for a volume fraction of 0.03% in the presence of magnetic field. The enhancement in the thermal conductivity has been observed for other volume fractions also. The increase in the thermal conductivity of these nanofluids can be attributed to the chain formation of magnetic nanomaterials in the base fluid in the presence of magnetic field. © *2011 American Institute of Physics*. [doi:10.1063/1.3642974]

I. INTRODUCTION

Nanofluids research is one of the emerging fields in nanotechnology application because of its wide use in the electronics and automobile industries. The commonly used nanomaterials for making nanofluids are Al_2O_3, CuO, TiO_2, Cu, carbon nanotubes (CNTs), graphene, etc.[1–5] The type of dispersant can change the property of a nanofluid and, thereby, the application. Magnetic nanofluids are a class of nanofluids made by dispersing magnetic nanomaterials such as Fe_2O_3, Fe_3O_4, and $CoFe_2O_4$ in a base fluid.[6–8] Magnetic nanofluids have broad applications in rotating seals or bearings in magnetic field. De-ionized (DI) water based magnetic nanofluids are mainly useful in biomedical applications, including magnetic cell separation, drug delivery, hyperthermia, and magnetic resonance imaging.[9]

The limited number of thermal conductivity studies on magnetic nanofluids is a result of the difficulty in making stable nanofluids.[9–12] In the absence of a proper surface coating, hydrophobic interactions between the nanoparticles will cause them to aggregate and form large clusters, resulting in an increased particle size. This can be avoided via the use of surfactants. However, in some cases the use of surfactants negatively affects the thermal conductivity of the nanofluid. In recent years, considerable efforts have been devoted to the design and controlled fabrication of nanostructured materials that display specific functional properties. Alternatively, organic compounds have often been employed in order to passivate the surface of the magnetic nanoparticles during or after the preparation procedure so as to avoid agglomeration. For example, organic compounds coated on iron oxide nanoparticles have been found to preserve the magnetic properties of iron oxides as well as exhibit the properties of organic molecules, and they therefore have potential applications in several areas.[13–16] Similarly, previous reports on the thermal conductivity enhancement of nanofluids with inorganic compounds suggest that those materials also can be used for coolant applications.[17–19] Chen *et al.*[20] reported that when the particle size of SiO_2 nanoparticles increases, the thermal conductivity of the corresponding fluid increases.

Owing to special properties such as a high thermal conductivity, a high aspect ratio, and good mechanical strength, CNTs are considered as good candidates for nanofluids. The thermal and magnetic properties of CNTs have been further improved by coating them with metals/metal oxides.[21,22] Wright *et al.*[22] have reported that Ni coated single walled carbon nanotubes (SWNTs) show excellent thermal behavior in the presence of magnetic field. The reason for this enhancement in the thermal conductivity is explained based on the alignment of the Ni coated SWNTs in the presence of magnetic field.

Philip *et al.*[23] have suggested that the chain formation of magnetic nanoparticles in the presence of magnetic field can increase the thermal transport property of magnetic nanofluids. Considering the special property of the enhancement of thermal conductivity in the presence of magnetic field, in the present work we have studied the thermal conductivity of Fe_3O_4 decorated multiwalled carbon nanotubes (MWNTs) (Fe_3O_4/MWNTs) without and with a SiO_2 coating. SiO_2 coating and functional groups present on the MWNTs give the proper dispersion of magnetic nanotubes in polar solvents without surfactant. In comparison with surfactant-coated nano-sized magnetite (NSM) particles, silica-coated

[a)]Author to whom correspondence should be addressed. Electronic mail: ramp@iitm.ac.in. FAX: +91-44-22570509.

FIG. 1. (Color online) Experimental setup used for the measurement of the thermal conductivity of the magnetic nanofluid in the presence of magnetic field.

NSM particles have some distinct advantages, including (a) no interference with the NSM's applications in medical and biological environments, (b) limited particle aggregation in solution, (c) improved chemical stability, and (d) easy surface modification with coupling agents. For comparison, the thermal conductivity of Fe_2O_3/MWNTs is also carried out.

II. MATERIALS AND METHODS

The synthesis of Fe_3O_4/MWNTs and Fe_3O_4@SiO_2/MWNTs is described elsewhere.[24] Briefly, MWNTs were synthesized via catalytic chemical vapor deposition over an alloy hydride catalyst and were purified by means of air oxidation and acid treatment. The purified MWNTs were first decorated with Fe_3O_4 nanoparticles via chemical reduction using hydrated ferric chloride and ferrous sulfate as precursors. Core-shell Fe_3O_4@SiO_2/MWNT nanoparticles were prepared by growing silica layers onto the surface of the Fe_3O_4/MWNTs via a chemical reduction technique. Tetraethoxysilane was used as the precursor for silica. Raman spectra were obtained using a WITEC alpha 300 Confocal Raman system equipped with a Nd:YAG laser (532 nm) as the excitation source. The intensity was kept at a minimum so as to avoid laser induced heating. Thermogravimetric analysis (TGA) studies were carried out using a Perkin Elmer TGA 6 analyzer. The morphology of the samples was characterized via field emission scanning electron microscopy (FESEM) (FEI QUANTA). Transmission electron microscopy (TEM) was carried out using a JEOL JEM-2010 F microscope. For the TEM measurements, samples were dispersed in absolute ethanol using mild ultrasonication and casted onto carbon coated Cu grids (SPI supplies, 200 mesh). The thermal conductivity of these fluids with magnetic field has been studied using the setup shown in Fig. 1. The setup consists of an electromagnet, a constant current source, and a Gauss meter. The distance between the poles of the electromagnet is about 5 cm. The sensor head inserted at the center of the sample bottle is placed at the middle of the poles. The magnetic field distribution between the poles is nearly uniform, and therefore the position of the sample bottle between the poles is not very important, but the sample bottle should be steady between the poles. The thermal conductivity of the nanofluids was measured using a KD2 Pro thermal properties analyzer (Decogon devices, USA). The KD2 Pro uses a transient heated needle to measure the thermal properties of the fluid media. The direction of the magnetic field was perpendicular to the plane of the rods (poles). The thermal conductivity measurement was performed along the direction of the magnetic field.

III. RESULTS AND DISCUSSION

The morphology and structure of the MWNTs were analyzed using TEM images and Raman spectra, respectively. The TEM image in Fig. 2(a) shows purified MWNTs of nearly uniform diameter. The diameter of the nanotubes varies between 30 to 40 nm. The Raman spectrum of purified MWNTs in Fig. 2(b) shows a peak at about 1569 cm^{-1} called the G-band, which is a characteristic of most of the graphitic materials. The D-band peak at 1339 cm^{-1} is due to the defects and disorder in the system.[25] The peak at 2675 cm^{-1} is the 2 D-band, which is the second order harmonic of the D-band. Figure 3(a) shows the Raman spectra of Fe_3O_4/MWNTs and Fe_3O_4@SiO_2/MWNTs. The peaks at about 1326 cm^{-1} and 1580 cm^{-1} correspond to the D-band and G-band vibrations, respectively. The shift in the D- and G-band peak positions of Fe_3O_4/MWNTs and Fe_3O_4@SiO_2/MWNTs is also confirmation of the decoration of

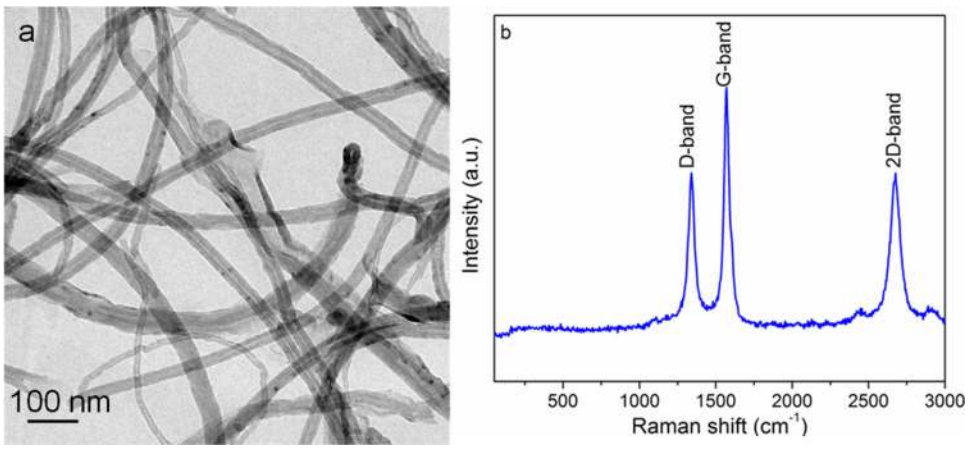

FIG. 2. (Color online) (a) TEM image and (b) Raman spectrum of purified MWNTs.

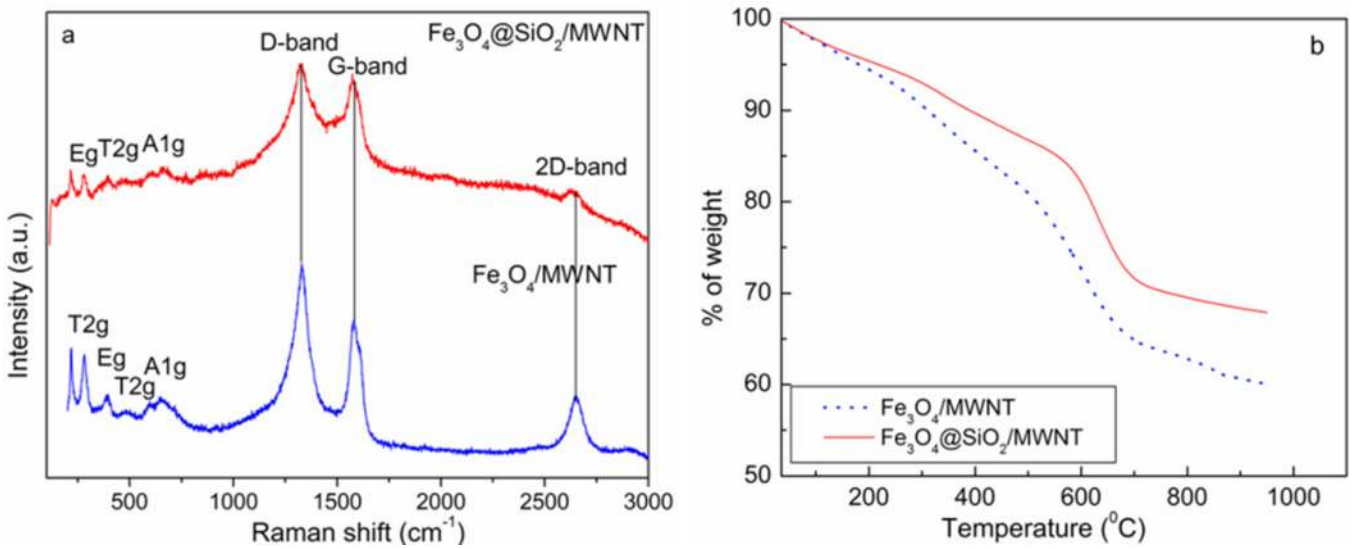

FIG. 3. (Color online) (a) Raman spectra and (b) thermogravimetric analysis of Fe_3O_4/MWNTs and Fe_3O_4@SiO_2/MWNTs.

nanoparticles on the MWNTs. The peaks below 1000 cm^{-1} in general represent the presence of oxides.[26–28] In the present case, the Fe_3O_4/MWNTs show peaks corresponding to Fe-O asymmetric bending T2g at about 281 and 591 cm^{-1}, Fe-O symmetric bending at about 393 cm^{-1} Eg, and Fe-O symmetric stretching at about 644 cm^{-1} A1g.[29] In the case of Fe_3O_4@SiO_2/MWNTs, the peak positions are slightly shifted compared to those of Fe_3O_4/MWNTs due to the SiO_2 coating. The thermal stability of the samples was studied using TGA in air atmosphere and is given in Fig. 3(b). The drastic weight loss in the TGA of Fe_3O_4/MWNTs and Fe_3O_4@SiO_2/MWNTs around 550 °C is due to the decomposition of the MWNTs. The small weight loss before this temperature is due to the removal of water and functional groups from the material.[30] The material left behind in the sample holder at 700 °C is due to the residual oxide nanoparticles. In

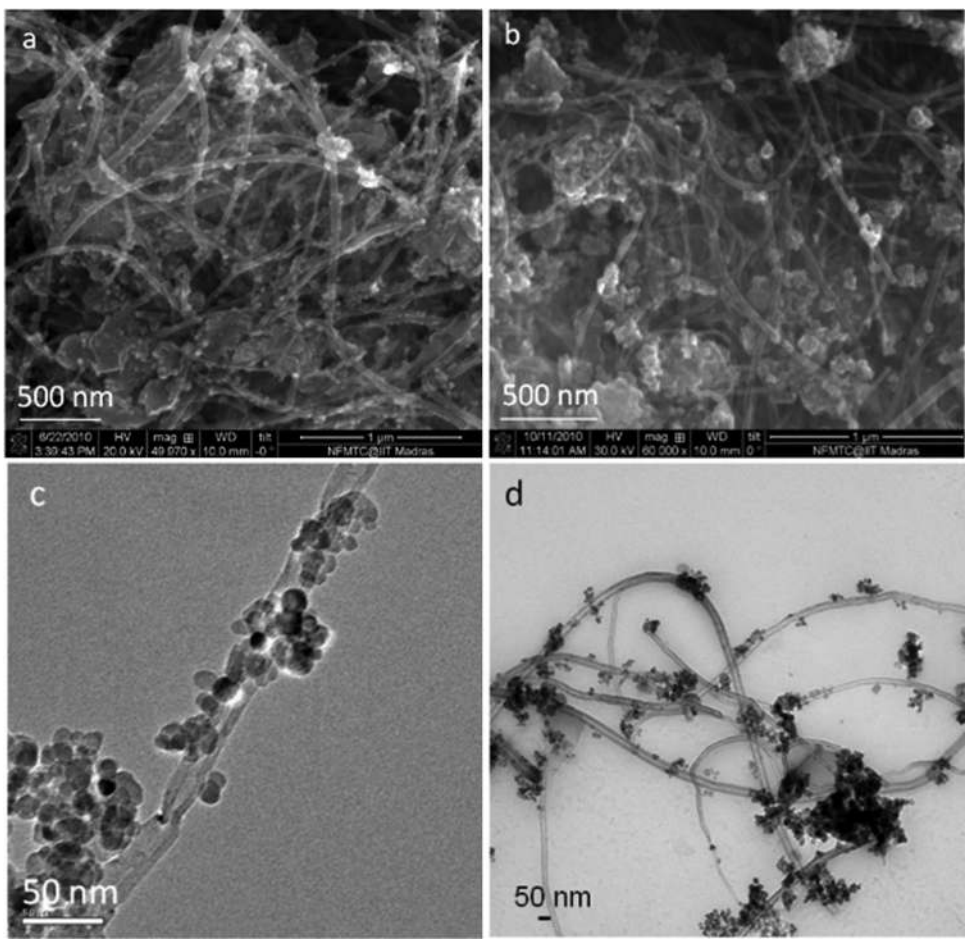

FIG. 4. (a),(b) Field emission scanning electron microscopy images of Fe_3O_4/MWNTs and Fe_3O_4@SiO_2/MWNTs. (c),(d) Transmission electron microscopy images of Fe_3O_4/MWNTs and Fe_3O_4@SiO_2/MWNTs.

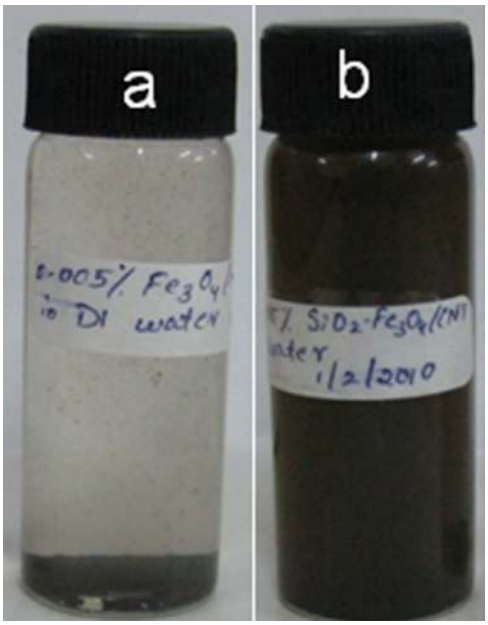

FIG. 5. (Color online) Photograph of (a) Fe_3O_4/MWNT and (b) Fe_3O_4@SiO_2/MWNT nanofluid (in DI water) without surfactant. The photograph was taken after one week of the synthesis.

the TGA of Fe_3O_4/MWNTs, the weight of the residue is about 60%. This suggests that Fe_3O_4/MWNTs contain 60% Fe_3O_4 nanoparticles. Because the same Fe_3O_4/MWNTs are used to make the Fe_3O_4@SiO_2/MWNTs, the residue left at 700 °C is due to Fe_3O_4 and SiO_2. The weight loss of Fe_3O_4@SiO_2/MWNTs at 700 °C is about 32%, i.e., the remaining 68% is Fe_3O_4 and SiO_2. Given that the Fe_3O_4 content is known to be 60% from the first curve, the other 8% is SiO_2.

FESEM [Figs. 4(a) and 4(b)] and TEM [Figs. 4(c) and 4(d)] images of Fe_3O_4/MWNTs and Fe_3O_4@SiO_2/MWNTs show the surface morphology of the nanomaterials. Nanoparticles are decorated on the MWNTs nearly uniformly. Fe_3O_4/MWNT dispersed nanofluid is made by dispersing a specific quantity of Fe_3O_4/MWNTs in DI water with 100 μl of oleic acid via ultrasonic irradiation. The same procedure is followed to make Fe_3O_4@SiO_2/MWNT dispersed nanofluids, without oleic acid. Figure 5 shows photographs of (a) Fe_3O_4/MWNTs and (b) Fe_3O_4@SiO_2/MWNTs in DI water based fluid without surfactant. The photographs are taken after one week of the synthesis. The Fe_3O_4/MWNT nanofluid settled nearly completely in this period of time, but no considerable settling is observed in the case of the Fe_3O_4@SiO_2/MWNT nanofluid.

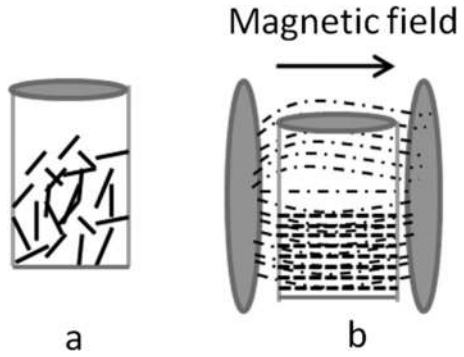

FIG. 7. Sample bottle (a) without magnetic field and (b) with magnetic field.

Figure 6(a) shows the thermal conductivity of the Fe_3O_4/MWNT nanofluids with respect to the temperature for different V_f without magnetic field. The enhancement of the thermal conductivity is calculated using the relation

$$\%\ enhancement = \frac{(k_n - k_f)}{k_f} \times 100,$$

where k_f is the thermal conductivity of the base fluid and k_n is that of the nanofluid. Fe_3O_4/MWNT dispersed DI water based nanofluid with a V_f of 0.005% shows an enhancement in thermal conductivity of about 3% at 30 °C and 5% at 50 °C. For 0.03% V_f, the enhancement is about 6.5% at 30 °C and 10% at 50 °C. The thermal conductivity increases with respect to both the volume fraction and the temperature. The increase in the thermal conductivity enhancement with respect to the temperature has been associated with an increase in the Brownian motion of the nanoparticles.[31] The enhancement in the thermal conductivity is not linear with the temperature and volume fraction; this is in agreement with previous reports.[32–34]

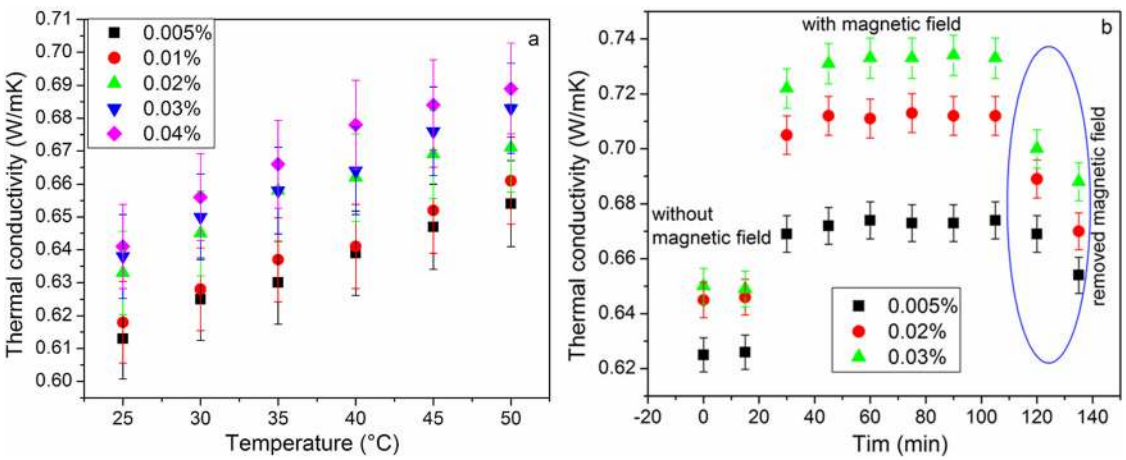

FIG. 6. (Color online) Thermal conductivity of Fe_3O_4/MWNTs (a) without magnetic field and (b) with magnetic field for different volume fractions.

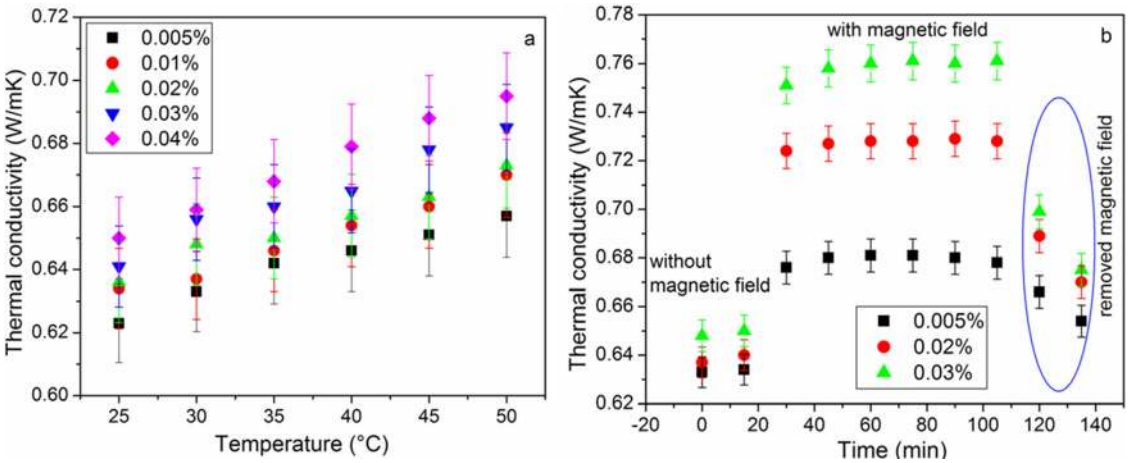

FIG. 8. (Color online) Thermal conductivity of Fe_3O_4@SiO_2/MWNTs (a) without magnetic field and (b) with magnetic field for different volume fractions.

The thermal conductivity of these fluids with magnetic field is given in Fig. 6(b). The magnetic fluid is kept between the poles of an electromagnet, and the thermal conductivity is measured with a constant magnetic field of ~80 G. The initial two points correspond to the thermal conductivity of the magnetic nanofluid at 30 °C without magnetic field. The points after that represent measurements in the presence of magnetic field. The thermal conductivity was measured in 15-minute intervals. The thermal conductivity increased tremendously in the presence of magnetic field, and the enhancement in the thermal conductivity is calculated using Eq. (1). In the presence of magnetic field, the enhancement in the thermal conductivity is about 10% for a 0.005% volume fraction and 20% for a 0.03% volume fraction. As reported by Philip *et al.*,[23] this enhancement can be due to the chain formation of magnetic MWNTs. The direction of the field is given in Fig. 7. Figure 7(a) shows the sample bottle without magnetic field; the nanomaterials are randomly oriented. But Fig. 7(b) shows the sample bottle in the presence of magnetic field; the magnetic nanomaterials are trying to align in the direction of the magnetic field, which helps with proper conduction. Though the enhancement in the thermal conductivity is less than that of Fe_3O_4 nanofluids,[23] it is nearly comparable to that of Ni coated SWNT nanofluids.[22] When the field is switched off, the thermal conductivity starts decreasing due to the settling and segregation of the Fe_3O_4/MWNTs. However, after ultrasonication, the fluid again becomes a magnetic nanofluid, and the thermal conductivity is nearly the same.

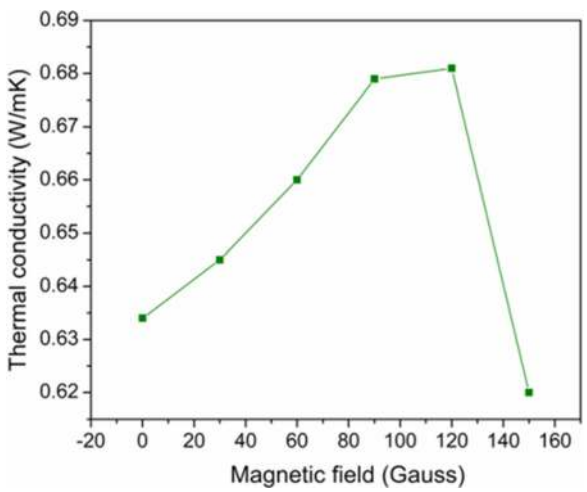

FIG. 9. (Color online) Study of the thermal conductivity of a 0.005% volume fraction of Fe_3O_4@SiO_2/MWNT dispersed nanofluid with varying magnetic fields.

Well-stabilized magnetic nanofluid has been synthesized using Fe_3O_4@SiO_2/MWNTs. The thermal conductivity measurement performed on Fe_3O_4@SiO_2/MWNT magnetic nanofluid is shown in Fig. 8. The thermal conductivity of Fe_3O_4@SiO_2/MWNT nanofluid without magnetic field for different V_f at different temperatures is given in Fig. 8(a). In this case, again the thermal conductivity increases with respect to the temperature and the V_f. The enhancement in the thermal conductivity is slightly higher than that of Fe_3O_4/MWNT nanofluid. The enhancement in the thermal conductivity is around 3.7% for 0.005% V_f at 30 °C and ~6% at 50 °C. Similarly, the enhancement is about 7.5% at 30 °C and ~10.5% at 50 °C for 0.03% V_f. The effect of magnetic field on this nanofluid is shown in Fig. 8(b). With magnetic field, the magnetic nanofluid shows an enhancement in its thermal conductivity of around 11.6% for 0.005% V_f and 24.5% for 0.03% V_f. Also in this case, when the magnetic field was removed, the thermal conductivity started decreasing. However, when the magnetic field was increased to a high value of about 130 G, the particles started agglomerating in the base fluid. Figure 9 shows the measurement of the thermal conductivity of the Fe_3O_4@SiO_2/MWNT nanofluid under different magnetic fields with a 0.005% V_f of Fe_3O_4@SiO_2/MWNTs. This suggests that by applying a high magnetic field to magnetic nanofluids, one can separate out magnetic nanoparticles from the base fluid. Because the maximum thermal conductivity enhancement is observed around the range of 80–120 G, the thermal conductivity measurements have been performed in a magnetic field of about 80 G.

IV. CONCLUSION

In summary, the thermal conductivity of Fe_3O_4/MWNT and Fe_3O_4@SiO_2/MWNT DI water based nanofluids has

been measured with and without magnetic field. Enhancements in the thermal conductivity of 20% and 24.5% have been achieved for a volume fraction of 0.03% Fe_3O_4@SiO_2/MWNTs at 30 °C. The enhancement in the thermal conductivity is due to the chain formation of magnetic MWNTs in the presence of magnetic field. The enhancement in the thermal conductivity suggests that these nanofluids can be used for coolant, sealing, and biomedical applications. Though there is an enhancement in the thermal conductivity, investigations of the effect of the base fluid and optimization of the volume fraction and temperature with magnetic field are further warranted.

ACKNOWLEDGMENTS

The authors wish to thank Defense Research and Development Organization (DRDO) and Indian Institute of Technology Madras (IITM), India, for financial support.

[1]S. Lee, S. U. S. Choi, S. Li, and J. A. Eastman, J. Heat Transfer **121**, 280 (1999).
[2]A. Turgut, I. Tavman, M. Chirtoc, H. P. Schuchmann, C. Sauter, and S. Tavman, Int. J. Thermophys. **30**, 1213 (2009).
[3]M. S. Liu, M. C. C. Lin, C. Y. Tsai, and C. C. Wang, Int. J. Heat Mass Transfer **49**, 3028 (2006).
[4]H. Xie and L. Chen, J. Chem. Eng. Data **56**, 1030 (2011).
[5]T. T. Baby and S. Ramaprabhu, J. Appl. Phys. **108**, 124308 (2010).
[6]S.-Z. Guo, Y. Li, J.-S. Jiang, and H.-Q. Xie, Nano. Res. Lett. **5**, 1222 (2010).
[7]M. Abareshi, E. K. Goharshadi, S. M. Zebarjad, H. K. Fadafan, and A. Youssefi, J. Magn. Magn. Mater. **322**, 3895 (2010).
[8]D. Dadarlat, C. Neamtu, M. Streza, R. Turcu, I. Craciunescu, D. Bica, and L. Vekas, J. Nanopart. Res. **10**, 1329 (2008).
[9]C.-K. Huang, C.-H. Hou, C.-C. Chen, Y.-L. Tsai, L.-M. Chang, H.-S. Wei, K.-H. Hsieh, and C.-H. Chan, Nanotechnology **19**, 055701 (2008).
[10]B. Zhao and Z. Nan, Nano. Res. Lett. **6**, 230 (2011).
[11]T.-H. Tsai, P.-H. Chen, D.-S. Lee, and C.-T. Yang, Nano. Res. Lett. **6**, 264 (2011).
[12]P. D. Shima, J. Philip, and B. Raj, J. Phys. Chem. C **114**, 18825 (2010).
[13]B. Basly, D. Felder-Flesch, P. Perriat, G. Pourroy, and S. Bégin-Colin, Contrast Media & Molecular Imaging **6**, 132 (2011).
[14]Y. Sahoo, A. Goodarzi, M. T. Swihart, T. Y. Ohulchanskyy, E. P. Furlani, and P. N. Prasad, J. Phys. Chem. B **109**, 3879 (2005).
[15]H. Xia, J. Yi, P. Foo, and B. Liu, Chem. Mater. **19**, 4087 (2007).
[16]J. Zhang, S. Xu, and E. Kumacheva, J. Am. Chem. Soc. **126**, 7908 (2004).
[17]D. Kwek, A. Crivoi, and F. Duan, J. Chem. Eng. Data **55**, 5690 (2010).
[18]D. V. Kuznetsov, S. P. Bardakhanov, A. V. Nomoev, S. A. Novopashin, and V. Z. Lygdenov, J. Eng. Thermophys. **19**, 138 (2010).
[19]H. Ahmari and S. G. Etemad, Rheol. Acta **48**, 217 (2009).
[20]G. Chen, W. Yu, D. Singh, D. Cookson, and J. Routbort, J. Nanopart. Res. **10**, 1109 (2008).
[21]J. Wensel, B. Wright, D. Thomas, W. Douglas, B. Mannhalter, W. Cross, H. Hong, J. Kellar, P. Smith, and W. Roy, Appl. Phys. Lett. **92**, 023110 (2008).
[22]B. Wright, D. Thomas, H. Hong, L. Groven, J. Puszynski, E. Duke, X. Ye, and S. Jin, Appl. Phys. Lett. **91**, 173116 (2007).
[23]J. Philip, P. D. Shima, and B. Raj, Appl. Phys. Lett. **91**, 203108 (2007).
[24]T. T. Baby and S. Ramaprabhu, Talanta **80**, 2016 (2010).
[25]M. S. Dresselhaus, G. Dresselhaus, R. Saito, and A. Jorio, Phys. Rep. **409**, 47 (2005).
[26]H. Jeziorowski and H. Knózinger, Chem. Phys. Lett. **42**, 162 (1976).
[27]F. Dumitrachea, I. Morjana, R. Alexandrescua, V. Ciupinab, G. Prodanb, I. Voicua, C. Fleacaa, L. Albua, M. Savoiua, I. Sandua, E. Popovicia, and I. Soarea, Appl. Surf. Sci. **247**, 25 (2005).
[28]S. S. Chan, I. E. Wachs, L. L. Murrell, L. Wang, and W. K. Hall, J. Phys. Chem. **88**, 5831 (1984).
[29]M. A. Legodi and D. de Waal, Dyes Pigm. **74**, 161 (2007).
[30]B. P. Ramesh, W. J. Blau, P. K. Tyagi, D. S. Misra, N. Ali, J. Gracio, G. Cabral, and E. Titus, Thin Solid Films **494**, 128 (2006).
[31]S. K. Das, N. Putra, P. Thiesen, and W. Roetzel, ASME J. Heat Transfer **125**, 567 (2003).
[32]Y. J. Hwang, Y. C. Ahn, H. S. Shin, C. G. Lee, G. T. Kim, H. S. Park, and J. K. Lee, Curr. Appl. Phys. **6**, 1068 (2006).
[33]M. S. Liu, M. C. C. Lin, I. T. Huang, and C. C. Wang, Int. Commun. Heat Mass Transfer **32**, 1202 (2005).
[34]D. S. Wen and Y. L. Ding, J. Thermophys. Heat Transfer **18**, 481 (2004).